J|A|C|S
ARTICLES
Published on Web 03/01/2002

Comprehensive Thermodynamic Characterization of the Metal−Hydrogen Bond in a Series of Cobalt-Hydride Complexes

Rebecca Ciancanelli,[†] Bruce C. Noll,[†] Daniel L. DuBois,*[,‡] and M. Rakowski DuBois*[,†]

Contribution from the Department of Chemistry and Biochemistry, University of Colorado, Boulder, Colorado 80309, and National Renewable Energy Laboratory, 1617 Cole Boulevard, Golden, Colorado 80401

Received October 1, 2001. Revised Manuscript Received January 14, 2002

Abstract: A detailed structural and thermodynamic study of a series of cobalt-hydride complexes is reported. This includes structural studies of $[H_2Co(dppe)_2]^+$, $HCo(dppe)_2$, $[HCo(dppe)_2(CH_3CN)]^+$, and $[Co(dppe)_2(CH_3CN)]^{2+}$, where dppe = bis(diphenylphosphino)ethane. Equilibrium measurements are reported for one hydride- and two proton-transfer reactions. These measurements and the determinations of various electrochemical potentials were used to determine 11 of 12 possible homolytic and heterolytic solution Co−H bond dissociation free energies of $[H_2Co(dppe)_2]^+$ and its monohydride derivatives. These values provide a useful framework for understanding observed and potential reactions of these complexes. These reactions include the disproportionation of $[HCo(dppe)_2]^+$ to form $[Co(dppe)_2]^+$ and $[H_2Co(dppe)_2]^+$, the reaction of $[Co(dppe)_2]^+$ with H_2, the protonation and deprotonation reactions of the various hydride species, and the relative ability of the hydride complexes to act as hydride donors.

Introduction

Transition metal hydrides are important intermediates in a wide range of catalytic reactions, and a more complete understanding of the M−H bond is important to the rational development of new catalysts and new catalytic processes. The metal−hydride bond can be cleaved in three different ways − by loss of a proton, a hydrogen atom, or a hydride anion, Scheme 1. Any of the reactions or combination of reactions shown in the scheme may be important for both stoichiometric and catalytic reactions.

Quantitative information on the energetics of these three possible reaction pathways can provide insights into the chemical reactivity and physical properties of these complexes, and can be quite useful in selecting appropriate conditions to carry out a desired chemical reaction. For example, the stereochemistry for the addition of metal hydrides to activated olefins is dependent on whether the hydride or its conjugate base is undergoing the reaction.[1] Similarly the catalytic hydroformylation of alkenes or hydrogenation of ketones involve a metal-hydride species,[2a,b] but the conjugate base of a hydride is the active catalyst in certain C−C bond cleavage reactions.[2c] The homolytic bond dissociation energies of metal hydrides and hydroxides are critical to our understanding of C−H bond activation reactions by metal radicals and metal-oxo complexes.[3] Finally, the hydride donor abilities of metal hydrides have been used to predict the heterolytic activation of hydrogen[4] and the reduction of carbonyl complexes to formyl complexes.[5]

Scheme 1

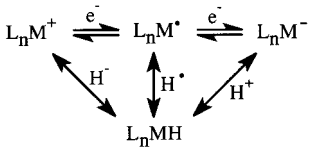

Most previous thermodynamic studies of transition metal hydrides have focused on a single type of bond cleavage reaction.[6−8] However, all three reactions shown in Scheme 1 are related to each other by the electron-transfer reactions indicated.[9] As one traverses Scheme 1 from left to right, the

[†] University of Colorado.
[‡] National Renewable Energy Laboratory.

(1) (a) Pattenden, G. *Chem. Soc. Rev.* **1988**, *17*, 361. (b) Schrauzer, G. N.; Windgassen, R. J. *J. Am. Chem. Soc.* **1967**, *89*, 1999.
(2) (a) Kollar, K.; Sandor, P.; Szalontai, G.; Heil, B. *J. Organomet. Chem.* **1990**, *393*, 153. (b) Linn, D.; Halpern, J. *J. Am. Chem. Soc.* **1987**, *109*, 2969−2974. (c) Hou, Z.; Koizumi, T.; Fujita, A.; Yamazaki, H.; Wakatsuki, Y. *J. Am. Chem. Soc.* **2001**, *123*, 5812−5813.
(3) (a) Wei, M.; Wayland, B. B. *Organometallics* **1996**, *15*, 4681−4683 and references therein. (b) Mayer, J. M. *Acc. Chem. Res.* **1998**, *31*, 441−450.
(4) (a) Berning, D. E.; Noll, B. C.; DuBois, D. L. *J. Am. Chem. Soc.* **1999**, *121*, 11432−11447. (b) Curtis, C. J.; Miedaner, A.; Ellis, W. W.; DuBois, D. L. *J. Am. Chem. Soc.* **2002**, *124*, ASAP (Feb. 21, 2002).
(5) Ellis, W. W.; Miedaner, A.; Curtis, C. J.; Gibson, D. H.; DuBois, D. L. *J. Am. Chem. Soc.* **2002**, *124*, in press.
(6) Some studies dealing primarily with pK_a measurements are: (a) Kristjánsdóttir, S. S.; Norton, J. R. In *Transition Metal Hydrides: Recent Advances in Theory and Experiment*; Dedieu, A., Ed.; VCH: New York, 1991; pp 309−359. (b) Jordan, R. F.; Norton, J. R. *J. Am. Chem. Soc.* **1982**, *104*, 1255−1263. (c) Moore, E. J.; Sullivan, J. M.; Norton, J. R. *IBID* **1986**, *108*, 2257−2263. (d) Kristjánsdóttir, S. S.; Moody, A. E.; Weberg, R. T.; Norton, J. R. *Organometallics* **1988**, *7*, 1983−1987. (e) Jessop, P. G.; Morris, R. H. *Coord. Chem. Rev.* **1992**, *121*, 155. (f) Bullock, R. M.; Song, J.-S.; Szalda, D. J. *Organometallics* **1996**, *15*, 2504−2516. (g) Davies, S. C.; Henderson, R. A.; Hughes, D. L.; Oglieve, K. E. *J. Chem. Soc., Dalton Trans.* **1998**, 425−431. (h) Abdur-Rashid, K.; Fong, T. P.; Greaves, B.; Gusev, D. G.; Hinman, J. G.; Landau, S. E.; Lough, A. J.; Morris, R. H. *J. Am. Chem. Soc.* **2000**, *122*, 9155−9171.

10.1021/ja0122804 CCC: $22.00

metal complexes are sequentially reduced by one electron, and the hydride ion is sequentially oxidized. We have recently measured the free energies associated with these three bond cleavage reactions for a series of $[HNi(diphosphine)_2]^+$ complexes.[3,4] In this paper we demonstrate that thermochemical cycles similar to the one shown in Scheme 1 can be extended to dihydride systems to provide a nearly comprehensive thermodynamic description of these systems as well. By using $[H_2Co(dppe)_2]^+$ as an example of a dihydride system, the set of reactions shown in Scheme 1 can be expanded to include the effects of oxidation on the different bond cleavage reactions of monohydride species. In addition, sequential bond cleavage reactions of dihydrides can be studied. These results provide the most comprehensive thermodynamic description developed to date for a transition metal-hydride system.

Results

Synthesis and Spectral Characterization of Co Complexes. The series of complexes $HCo(dppe)_2$, $[HCo(dppe)_2]^+$, and $[HCo(dppe)_2(CH_3CN)]^{2+}$ [11,12] (where dppe = bis(diphenylphosphino)-ethane) is particularly attractive for obtaining information on the effects of oxidation on the thermodynamics of the M−H bond, because they represent the sequential oxidation from Co(I) to Co(III). In addition, $[Co(dppe)_2(CH_3CN)]^{2+}$ and $[H_2Co(dppe)_2]^+$ are also known[12,13] and provide the opportunity for studying successive proton, hydrogen atom, and hydride-transfer reactions. The complexes were all synthesized by modifications of previous synthetic methods as described in the Experimental Section. A more complete spectral characterization is provided for the products, since several of the spectroscopic techniques were not routinely available when these complexes were first reported.

All of the diamagnetic hydride complexes have been characterized by ^{1}H and ^{31}P NMR spectroscopy. The hydride region of the ^{1}H NMR spectrum of $HCo(dppe)_2$ exhibits a broad quintet at −14.9 ppm. The quintet pattern arises from coupling to four equivalent phosphorus atoms. The equivalence of the four phosphorus atoms is also supported by the ^{31}P NMR spectrum which exhibits a single broad resonance at 72.9 ppm. As discussed below, the results of an X-ray diffraction study of this complex indicate a distorted trigonal bipyramidal structure with the hydride trans to one phosphorus atom and cis to three others. The apparent equivalence of the phosphorus atoms in the NMR spectra is attributed to a fluxional process. Fluxionality is common in five-coordinate d^8 complexes.[14]

The hydride ligand of $[HCo(dppe)_2(CH_3CN)]^{2+}$ also exhibits a broad quintet resonance (−21.1 ppm) in the ^{1}H NMR spectrum. In this case, the equivalence of the four phosphorus atoms is a result of the hydride ligand occupying a position that is cis to the four phosphorus atoms in a nonfluxional octahedral complex. Again a single broad resonance is observed in the ^{31}P NMR spectrum consistent with four equivalent nuclei.

The dihydride complex $[H_2Co(dppe)_2]^+$ has been assigned as the cis isomer on the basis of the NMR spectra. The resonance for the hydrides appears as two broad and overlapping quartets at −13.2 ppm in the ^{1}H NMR spectrum, and two broad resonances at 69.7 and 80.5 ppm are observed in the ^{31}P NMR spectrum. The ^{31}P NMR resonances for all the cobalt complexes are quite broad, and this is attributed to the quadrupole of the ^{59}Co nucleus which has a spin of $^7/_2$.

The paramagnetic Co(II) hydride $[HCo(dppe)_2]^+$ has been characterized by EPR spectroscopy. The spectrum, recorded in acetonitrile at room temperature, exhibited a doublet with a g value of 2.1 and a hyperfine coupling of 80 G. These results are consistent with the low-spin magnetic moment of 2.2 μ_B reported previously for this complex.[12] The data are similar to those observed for previously characterized trigonal bipyramidal complexes such as $[Co(PP_3)(CH_3CN)]^{2+}$ (g = 2.11, A = 90 G)[15] (where PP_3 is tris(diphenylphosphinoethyl)phosphine), $[HCo(PP_3)](PF_6)$, 2.01 μ_B,[16] and $HCo(CP_3)PEt_3](BPh_4)$ (where CP_3 is $CH_3C(CH_2PPh_2)_3$, 2.15 μ_B, and g = 2.20.[17]

Structural Studies. Single crystals of $HCo(dppe)_2$ and the cations $[Co(dppe)_2(CH_3CN)]^{2+}$, $[HCo(dppe)_2(CH_3CN)]^{2+}$, and $[H_2Co(dppe)_2]^+$ were characterized by X-ray diffraction, and perspective drawings of the neutral and cationic cobalt structures are shown in Figure 1. Tables 1 and 2 contain selected bond lengths and bond angles, respectively, for these complexes. It can be seen from Figure 1a that $HCo(dppe)_2$ is best described as a distorted trigonal bipyramidal complex with one phosphorus atom and the hydride occupying axial positions. The H1−Co−P1 bond angle for this complex is 163.2°. The deviation from 180° is caused by the small P1−Co−P2 angle (87.0°) typical of a chelating dppe ligand. The average of the three angles between the axial hydrogen atom and the three equatorial phosphorus atoms is 82.2°, significantly less than 90°. This bending of cis ligands toward hydrogen is expected for both steric and electronic reasons.[17] The four Co−P bond distances (2.12−2.16 Å, av = 2.15 Å) and the Co−H bond distance of1.46 Å are similar to values reported for other Co(I) hydrides.[15,16]

(7) Some studies dealing primarily with homolytic M−H bond cleavage are: (a) Simões, J. A. M.; Beauchamp, J. L. *Chem. Rev.* **1990**, *90*, 629−688. (b) Kiss, G.; Zhang, K.; Mukerjee, S. L.; Hoff, C. D. *J. Am. Chem. Soc.* **1990**, *112*, 5657−5658. (c) Schock, L. E.; Marks, T. J. *J. Am. Chem. Soc.* **1988**, *110*, 7701−7715. (d) Tilset, M.; Parker, V. D. *J. Am. Chem. Soc.* **1989**, *111*, 6711−6717. (e) *IBID* **1990**, *112*, 2843. (f) Parker, V. D.; Handoo, K. L.; Roness, F.; Tilset, M. *J. Am. Chem. Soc.* **1991**, *113*, 7493−7498. (g) Ryan, B. O.; Tilset, M.; Parker, V. D. *J. Am. Chem. Soc.* **1990**, *112*, 2618−2626.

(8) Some studies dealing primarily with the thermodynamics and kinetics of hydride transfer are: (a) Sarker, N.; Bruno, J. W. *J. Am. Chem. Soc.* **1999**, *121*, 2174−2180. (b) Labinger, J. A. In *Transition Metal Hydrides: Recent Advances in Theory and Experiment*; Dedieu, A., Ed.; VCH: New York, 1991; pp 361−379. (c) Labinger, J. A.; Komadina, K. H. *J. Organomet. Chem.* **1978**, *155*, C25−C28. (d) Kao, S. C.; Spillett, C. T.; Ash, C.; Lusk, R.; Park, Y. K.; Darensbourg, M. Y. *Organometallics* **1985**, *4*, 83−91. (e) Kao, S. C.; Gaus, P. L.; Youngdahl, K.; Darensbourg, M. Y. *Organometallics* **1984**, *3*, 1601−1603. (f) Gaus, P. L.; Kao, S. C.; Youngdahl, K.; Darensbourg, M. Y. *J. Am. Chem. Soc.* **1985**, *107*, 2428−2434. (g) Kinney, R. J.; Jones, W. D.; Bergman, R. G. *J. Am. Chem. Soc.* **1978**, *100*, 7902−7915. (h) Martin, B. D.; Warner, K. E.; Norton, J. R. *J. Am. Chem. Soc.* **1986**, *108*, 33−39. (i) Hembre, R. T.; McQueen, J. S. *Angew. Chem., Int. Ed. Engl.* **1997**, *36*, 65−67. (j) Hembre, R. T.; McQueen, S. *J. Am. Chem. Soc.* **1994**, *116*, 2141−2142. (k) Cheng, T.-Y.; Brunschwig, B. S.; Bullock, R. M. *J. Am. Chem. Soc.* **1998**, *120*, 13121−13137.

(9) These relationships are clearly presented in: Wayner, D. D. M.; Parker, V. D. *Acc. Chem. Res.* **1993**, *26*, 287−294.

(10) Berning, D. E.; Miedaner, A.; Curtis, C. J.; Noll, B. C.; Rakowski DuBois, M.; DuBois, D. L. *Organometallics* **2001**, *20*, 1832−1839.

(11) (a) Sacco, A.; Ugo, R. *J. Chem. Soc.* **1964**, 3274−3278. (b) Holah, D. G.; Hughes, A. N.; Maciaszek, S.; Magnuson, V. R.; Parker, K. O. *Inorg. Chem.* **1985**, *24*, 3956−3962. (c) Bianco, V. D.; Doronzo, S.; Gallo, N. *Inorg. Synth.* **1980**, *20*, 206−208.

(12) Pilloni, G.; Schiavon, G.; Zotti, G.; Zecchin, S. *J. Organomet. Chem.* **1977**, *134*, 305−318.

(13) DuBois, D. L.; Miedaner, A. *Inorg. Chem.* **1986**, *25*, 4642−4650.

(14) English, A. D.; Ittel, S. D.; Tolman, C. A.; Meakin, P.; Jesson, J. P. *J. Am. Chem. Soc.* **1977**, *99*, 117−120.

(15) (a) Bianchini, C.; Innocenti, P.; Meli, A.; Peruzzini, M.; Zanobini, F. *Organometallics* **1990**, *9*, 2514−2522. (b) Orlandini, A.; Sacconi, L. *Cryst. Struct. Commun.* **1975**, *4*, 157−161.

(16) Bianchini, C.; Masi, D.; Mealli, C.; Sabat, M. *Gazz. Chim. Ital.* **1986**, *116*, 201−206.

(17) (a) Elian, M.; Hoffmann, R. *Inorg. Chem.* **1975**, *14*, 1058−1076. (b) Wander, S. A.; Miedaner, A.; Noll, B. C.; Barkley, R. M.; DuBois, D. L. *Organometallics* **1996**, *15*, 3360−3373.

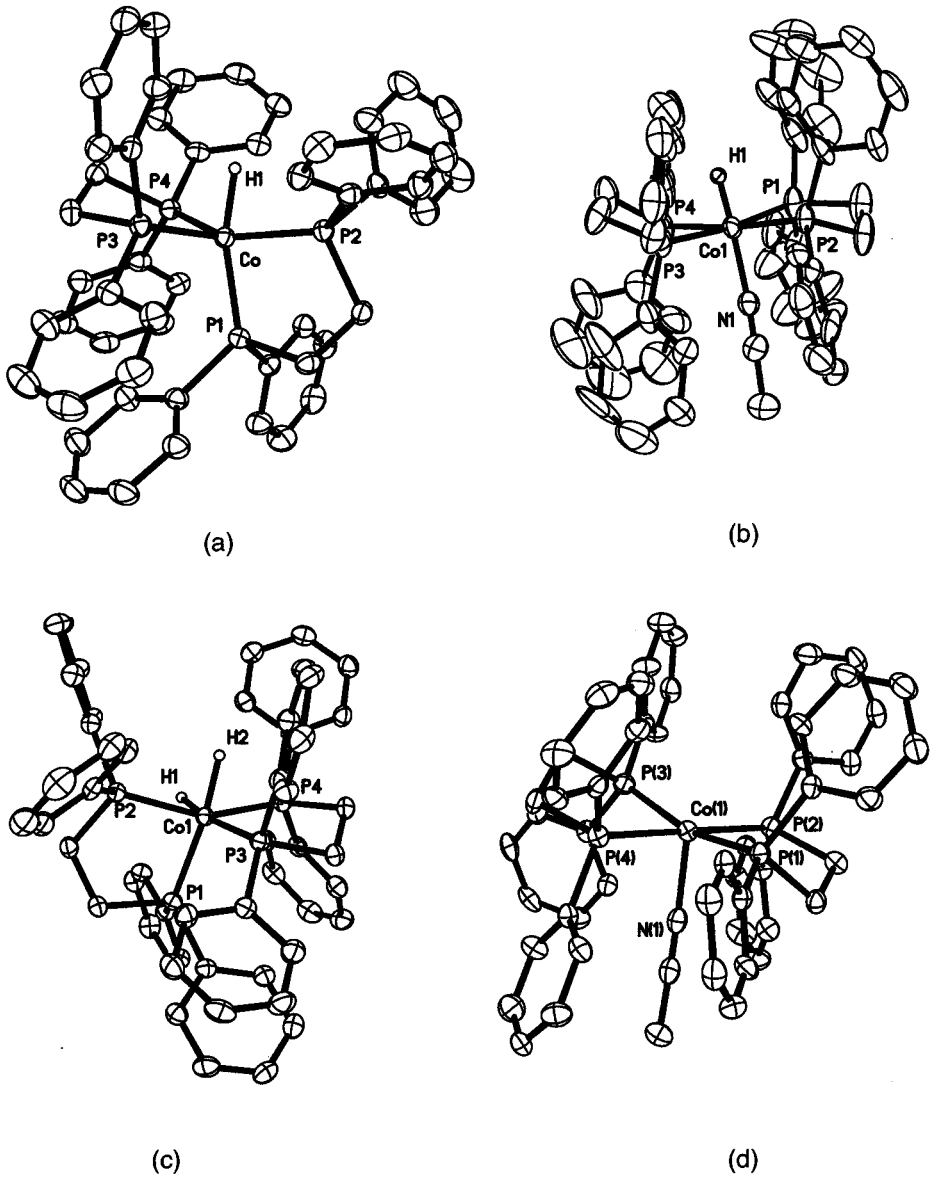

Figure 1. Ortep plots of (a) $HCo(dppe)_2$; (b) $[HCo(dppe)_2(CH_3CN)]^{2+}$; (c) $[H_2(Co(dppe)_2]^{+}$; (d) $[Co(dppe)_2(CH_3CN)]^{2+}$. Thermal ellipsoids are drawn at 50% probability.

Table 1. Selected Bond Distances (Å)

compd	M–P(1)	M–P(2)	M–P(3)	M–P(4)	M–N	M–H
$HCo(dppe)_2$	2.1519(5)	2.1242(5)	2.1623(5)	2.1523(5)		1.46(3)
$[HCo(dppe)_2CH_3CN][PF_6]_2$	2.278(2)	2.270(2)	2.295(2)	2.272(2)	1.929(8)	1.34(6)
$[H_2Co(dppe)_2][BF_4]$	2.2138(10)	2.1793(10)	2.2158(10)	2.1687(10)		1.42(3)
						1.47(4)
$[Co(dppe)_2CH_3CN][BF_4]_2$	2.2843(14)	2.2988(15)	2.3376(15)	2.3037(14)	2.017(4)	

The $[HCo(dppe)_2(CH_3CN)]^{2+}$ cation (Figure 1b) is an octahedron with trans hydride and acetonitrile ligands. The H1−Co−N1 bond angle of 173° is nearly linear, and the cis phosphorus ligands again bend away from the nitrogen atom of acetonitrile (average N−Co−P = 93.4°) toward the hydride ligand. The average Co−P bond distance (2.28 Å) is significantly longer than that observed for $HCo(dppe)_2$ discussed above, and the Co−N distance of 1.93 Å is less than that observed for $[Co(dppe)_2(CH_3CN)]^{2+}$ (2.02 Å) discussed below. The cationic dihydride complex, $[H_2Co(dppe)_2]^{+}$ (Figure 1c), has a distorted cis octahedral structure. The P−Co−P angles that are constrained by the chelate rings have angles near 90° (89.2° average), but the four remaining angles deviate significantly from the 180° and 90° expected for an ideal octahedral complex. This distortion is again a result of the movement of the phosphorus atoms toward the hydride ligands. The two Co−P bond distances for the phosphorus atoms that are trans to the hydride ligands are slightly longer than the Co−P distances for the two trans phosphorus atoms. The average Co−P bond distance for this complex (2.20 Å) is intermediate between those of $HCo(dppe)_2$ and $[HCo(dppe)_2(CH_3CN)]^{2+}$.

The $[Co(dppe)_2(CH_3CN)]^{2+}$ cation (Figure 1d) is best described as a square pyramid in which acetonitrile occupies the apex. Three of the four N−Co−P bond angles are very close

Table 2. Selected Bond Angles (deg)

			$HCo(dppe)_2$				
P(2)−Co−P(1)	86.98(2)	P(2)−Co−P(4)	137.95(2)	P(2)−Co−H(1)	78.1(11)	P(1)−Co−H(1)	163.2(11)
P(1)−Co−P(4)	107.72(2)	P(2)−Co−P(3)	123.41(2)	P(4)−Co−H(1)	79.2(11)	P(3)−Co−H(1)	89.2(10)
P(1)−Co−P(3)	105.67(2)	P(4)−Co−P(3)	91.06(2)				
			$[HCo(dppe)_2CH_3CN]^{2+}$				
N(1)−Co−P(2)	88.9(2)	N(1)−Co−P(4)	97.3(2)	P(4)−Co−P(3)	82.54(9)	P(1)−Co−P(3)	172.61(10)
P(2)−Co−P(4)	173.76(10)	N(1)−Co−P(1)	93.8(2)	N(1)−Co−H(1)	173(3)	P(2)−Co−H(1)	89(3)
P(2)−Co−P(1)	83.68(8)	P(4)−Co−P(1)	95.57(9)	P(4)−Co−H(1)	85(3)	P(1)−Co−H(1)	93(3)
N(1)−Co−P(3)	93.5(2)	P(2)−Co−P(3)	97.42(8)	P(3)−Co−H(1)	80(3)		
			$[H_2Co(dppe)_2]^+$				
P(4)−Co−P(2)	152.89(4)	P(4)−Co−P(1)	107.06(4)	P(1)−Co−H(1)	86.2(11)	P(3)−Co−H(1)	169.1(11)
P(2)−Co−P(1)	89.80(2)	P(4)−Co−P(3)	88.72(4)	P(4)−Co−H(2)	75.2(14)	P(2)−Co−H(2)	85.0(14)
P(2)−Co−P(3)	109.57(4)	P(1)−Co−P(3)	99.90(4)	P(1)−Co−H(2)	170.8(14)	P(3)−Co−H(2)	89.0(14)
P(4)−Co−H(1)	80.9(11)	P(2)−Co−H(1)	79.2(11)	H(1)−Co−H(2)	85.3(18)		
			$[Co(dppe)_2CH_3CN]^{2+}$				
N(1)−Co−P(1)	89.89(12)	N(1)−Co−P(2)	91.33(12)	N(1)−Co−P(3)	105.52(12)	P(1)−Co−P(3)	164.58(6)
P(1)−Co−P(2)	82.70(5)	N(1)−Co−P(4)	88.34(12)	P(2)−Co−P(3)	97.18(5)	P(4)−Co−P(3)	83.85(5)
P(1)−Co−P(4)	96.32(5)	P(2)−Co−P(4)	178.97(6)				

to 90° with the fourth angle being significantly larger at 105.5°. The Co−N bond length of 2.02 Å is 0.09 Å longer than that for $[HCo(dppe)_2(CH_3CN)]^{2+}$. This is attributed to the unpaired electron occupying an orbital with significant Co−N antibonding character for $[Co(dppe)_2(CH_3CN)]^{2+}$. The average Co−P bond length (2.30 Å) is the longest of the complexes studied and is consistent with an increase in the Co−P bond length as the charge on the complex increases, that is, $HCo(dppe)_2$ (2.15 Å) < $[H_2Co(dppe)_2]^+$ (2.20 Å) < $[HCo(dppe)_2(CH_3CN)]^{2+}$ (2.28 Å) < $[Co(dppe)_2(CH_3CN)]^{2+}$ (2.30 Å). This trend has been observed for a number of metal-phosphine complexes.[3,10,18] The trend would be consistent with either increased π back-bonding or increased M−L bond covalency as the positive charge decreases.

Electrochemical Studies. Electrochemical studies of $[Co(dppe)_2(CH_3CN)]^{2+}$ and $HCo(dppe)_2$ have been described previously.[12] However, these studies were performed in different solvents or solvent mixtures with different reference and working electrodes. To obtain accurate thermodynamic data, it is important to obtain all measurements under the same conditions. Therefore, we have repeated the cyclic voltammograms using acetonitrile and benzonitrile as solvents, glassy carbon as the working electrode, and the ferrocene/ferrocenium couple as an internal reference.[19]

A cyclic voltammogram of $[Co(dppe)_2(CH_3CN)]^{2+}$ in acetonitrile is shown in Figure 2, trace a. It consists of three reversible, diffusion-controlled, one-electron reductions at −0.70, −1.56, and −2.03 V, assigned to the Co(II/I), Co(I/0), and Co(0/−I) couples as reported previously. The separation between the cathodic and anodic peaks of each wave is near the 60 mV value expected for a reversible one-electron process. Because of the reversible nature of these one-electron processes, the thermodynamic data based on the values for these couples should be very reliable. As discussed above, the $[Co(dppe)_2(CH_3CN)]^{2+}$ cation is five-coordinate with a weakly bound acetonitrile ligand. This ligand is lost during the sequential reduction to the Co(−I) species. The ligand loss most likely occurs during the reduction from Co(II) to Co(I) as the latter

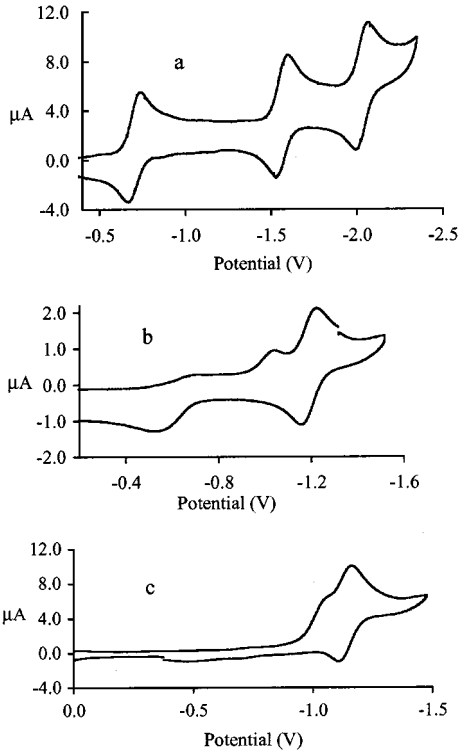

Figure 2. (a) Cyclic voltammogram of a 1×10^{-3} M solution of $[Co(dppe)_2(CH_3CN)][BF_4]_2$ in 0.3 M Bu_4NBF_4/acetonitrile. (b) Cyclic voltammogram of a 1×10^{-3} M solution of $HCo(dppe)_2$ in 0.3 M Bu_4NBF_4/benzonitrile. (c) Cyclic voltammogram of a 1×10^{-3} M solution of $[HCo(dppe)_2(CH_3CN)][PF_6]_2$ in 0.3 M Bu_4NBF_4/acetonitrile. In each case, the scan rate was 0.05 V/s, and the potentials are shown vs the ferrocene/ferrocenium couple.

d^8 species is expected to form a square-planar complex. The geometry of the square-planar Co(I) complex is expected to change to a distorted tetrahedron upon further reduction on the basis of the structures of other four-coordinate d^8, d^9, and d^{10} complexes.[3,10,18] These rearrangements are rapid on the CV time scale at scan rates of 50−1000 mV/sec.

The cyclic voltammograms of the cobalt(I)-, cobalt(II)-, and cobalt(III)-hydride derivatives have also been obtained. Studies of $HCo(dppe)_2$ were performed in benzonitrile because it is insoluble in acetonitrile. Studies of $[HCo(dppe)_2(CH_3CN)]^{2+}$ and $[HCo(dppe)_2]^+$ have been carried out in both benzonitrile and acetonitrile to confirm that the electrochemical responses are

(18) Longato, B.; Riello, L.; Bandoli, G.; Pilloni, G. *Inorg. Chem.* **1999**, *37*, 2818.
(19) (a) Gagné, R. R.; Koval, C. A.; Lisensky, G. C. *Inorg. Chem.* **1980**, *19*, 2854. (b) Gritzner, G.; Kuta, J. *Pure Appl. Chem.* **1984**, *56*, 462. (c) Hupp, J. T. *Inorg. Chem.* **1990**, *29*, 5010.

very similar in both solvents. Cyclic voltammograms of $HCo(dppe)_2$ and $[HCo(dppe)_2(CH_3CN)]^{2+}$ in benzonitrile and acetonitrile are shown by traces b and c of Figure 2. It can be seen that the HCo(I)/HCo(II) couple involves a reversible electron transfer near −1.2 V in both solvents. A second irreversible oxidation wave is observed at −0.53 V (50 mV/S scan rate in acetonitrile) that is assigned to the oxidation of $[HCo(dppe)_2]^+$ to form $[HCo(dppe)_2(CH_3CN)]^{2+}$. An irreversible cathodic peak at −1.02 V corresponding to the HCo(III)/HCo(II) reduction is associated with this wave.

Because the $[HCo(dppe)_2(CH_3CN)]^{2+}/[HCo(dppe)_2]^+$ couple is irreversible on the time scale of a cyclic voltammmetry experiment, its potential was determined from potentiometric measurements on acetonitrile solutions containing 50:50 mixtures of the isolated Co(III) and Co(II) hydride derivatives. If these measurements are made within 30 min after mixing fresh solutions of $[HCo(dppe)_2]^+$ and $[HCo(dppe)_2(CH_3CN)]^{2+}$, a stable and reproducible potential of −0.83 V is obtained. However, measurements taken over longer time periods of 1−2 h were irreproducible. Additional studies revealed that solutions of $[HCo(dppe)_2]^+$ slowly disproportionate upon standing in solution to form $[Co(dppe)_2]^+$ and $[H_2Co(dppe)_2]^+$ (reaction 1). The formation of $[Co(dppe)_2]^+$ can be followed by the slow

$$2[HCo(dppe)_2]^+ \rightarrow [H_2Co(dppe)_2]^+ + [Co(dppe)_2]^+ \quad (1)$$

appearance of the three cyclic voltammetric waves associated with this compound. Approximately 5% of the expected stoichiometric concentration of $[Co(dppe)_2]^+$ was observed in 1 h, and crystals of $[H_2Co(dppe)_2](PF_6)_2$ were isolated from acetone solutions of $[HCo(dppe)_2](PF_6)$ over a period of several days. Identical disproportionation reactions have been reported to be fast for $[HRh(dppe)_2]^+$ and $[HIr(dppe)_2]^+$.[12]

No reversible or quasi-reversible waves are observed for cyclic voltammograms of $[H_2Co(dppe)_2]^{2+}$ in acetonitrile solutions. As a result, it is not possible to obtain information on the effects of the oxidation state of Co on the Co−H bond cleavage energies for this dihydride complex.

Equilibrium Studies of Proton and Hydride Transfers. Reactions of the Co(III) hydride complexes with appropriate bases were studied to determine acid strengths of these complexes. For example, $[HCo(dppe)_2(CH_3CN)]^{2+}$ is deprotonated by anisidine in acetonitrile to form an equilibrium mixture as shown in reaction 2

$$[HCo(dppe)_2(CH_3CN)]^{2+} + B \leftrightarrows [Co(dppe)_2]^+ + BH^+ + CH_3CN \quad (2)$$

where

$$B = CH_3OC_6H_4NH_2$$

This reaction can be conveniently followed by ^1H NMR spectroscopy. Integration of the resonances of the methylene protons of the dppe ligand in each complex provides a convenient method for determining the ratios of $[HCo(dppe)_2(CH_3CN)]^{2+}$ and $[Co(dppe)_2]^+$. The ratios of protonated anisidine and anisidine were determined by using a large excess (approximately 10-fold) of each reagent in a predetermined ratio. Under these conditions, the deprotonation of $[HCo(dppe)_2(CH_3CN)]^{2+}$ makes a negligible contribution to the ratio of protonated and unprotonated anisidine. Integrations reached constant values over a period of 6 days. To confirm that the system is indeed at equilibrium, the reaction was also followed in the reverse direction, that is, starting from $[Co(dppe)_2]^+$. The results of these experiments gave the same value for the equilibrium constant within experimental error ($K_{eq\,2} = 1.0 \pm 0.2$). The pK_a value of $[HCo(dppe)_2(CH_3CN)]^{2+}$ in acetonitrile (11.3) can be determined by subtracting the log of the equilibrium constant for reaction 2 from the pK_a value of the anisidinium ion in the same solvent (11.3).[20]

Similarly, $[H_2Co(dppe)_2]^+$ reacts with tetramethylguanidine in acetonitrile-d_3 and benzonitrile solutions to form $HCo(dppe)_2$. Again, an excess of a mixture of tetramethylguanidine and its protonated form was used to establish a fixed ratio of these two species. In this case, the reaction was monitored by ^1H NMR spectroscopy using the hydride resonance of the two cobalt complexes. This reaction can also be studied by ^{31}P NMR spectroscopy. The reverse reaction was studied in benzonitrile because of the low solubility of $HCo(dppe)_2$ in acetonitrile. The equilibrium constant measured in acetonitrile for the deprotonation reaction (2.7 ± 0.3) is within experimental error of the value measured in benzonitrile for the reverse reaction (2.5). The pK_a value calculated for $[H_2Co(dppe)_2]^+$ in acetonitrile is 22.8 based on a pK_a value of 23.3 for protonated tetramethylguanidine.[21]

To determine the hydride donor ability of $HCo(dppe)_2$, attempts were made to observe equilibrium hydride-transfer reactions between $HCo(dppe)_2$ and $[Ni(diphosphine)_2]^{2+}$ complexes of known hydride acceptor ability. However, these studies were complicated by exchange of the diphosphine ligands and decomposition of some of the complexes during the course of the reaction. A different method was therefore used to determine the hydride donor ability of $[H_2Co(dppe)_2]^+$. Hydride donor values can also be obtained from equilibria involving the heterolytic cleavage of hydrogen in the presence of a base of known strength.[4] $[HCo(dppe)_2(CH_3CN)]^{2+}$ was found to react reversibly with hydrogen and 2,4-dichloroaniline to form $[H_2Co(dppe)_2]^+$ and 2,4-dichloroanalinium (pK_a = 8.0 in acetonitrile)[20] (reaction 3), and the equilibrium constant for reaction 3 ($K_{eq\,3} = 1.1 \pm 0.2$) was determined by NMR spectroscopy. The activity of hydrogen at 1.0 atm was taken as 1.0 in reaction 3 as this is the reference state for hydrogen for the normal hydrogen electrode.

$$[HCo(dppe)_2(CH_3CN)]^{2+} + B + H_2 \leftrightarrows [H_2Co(dppe)_2]^+ + BH^+ + CH_3CN \quad (3)$$

$$BH^+ \rightarrow B + H^+ \quad (4)$$

$$H^+ + H^- \rightarrow H_2 \quad (5)$$

$$[HCo(dppe)_2(CH_3CN)]^{2+} + H^- \rightarrow [H_2Co(dppe)_2]^+ + CH_3CN \quad (6)$$

$$\Delta G^\circ_{H^-} = -1.37pK_{eq\,3} - 1.37pK_{a(4)} + 76.0 \text{ kcal/mol} \quad (7)$$

(20) Edidin, R. T.; Sullivan, J. M.; Norton, J. R. *J. Am. Chem. Soc.* **1987**, *109*, 3945−3953.
(21) (a) Coetzee, J. F. *Prog. Phys. Org. Chem.* **1967**, *4*, 45. (b) Kolthoff, I. M.; Chantooni, M. K., Jr.; Bhowmik, S. *J. Am. Chem. Soc.* **1968**, *90*, 23−28. (c) Coetzee, J. F.; Padmanabhan, G. R. *J. Am. Chem. Soc.* **1965**, *87*, 5005.

Table 3. Thermodynamic Data ($\Delta G°$ Values in kcal/mol) for Cobalt-Hydride Derivatives

complex	pK_a	$\Delta G°_{H^+}$	$\Delta G°_{H\cdot}$	$\Delta G°_{H^-}$
$[H_2Co(dppe)_2]^+$	22.8	31.3	58.0	65.1
$HCo(dppe)_2$	38.1	52.3	59.1	49.1
$[HCo(dppe)_2]^+$	23.6	32.4	49.9	59.7
$[HCo(dppe)_2(CH_3CN)]^{+2}$	11.3	15.5	52.9	

Reaction 3 can be combined with reactions 4 and 5 to give information on the heterolytic cleavage of the Co−H bond of $[H_2Co(dppe)_2]^+$ in acetonitrile (the reverse of reaction 6). The free energies associated with reactions 3−5 can be used in eq 7 to calculate that the hydride donor ability, $\Delta G°_{H^-}$, of $[H_2Co(dppe)_2]^+$ is 65.1 kcal/mol.

Free Energy Relationships. The reduction potentials and equilibrium constants discussed above for the cobalt-dppe derivatives have been used to determine free energy values of the three different Co−H bond cleavage reactions for the four cobalt species as summarized in Table 3. Equations 8−11 show a thermodynamic cycle that can be used to calculate $\Delta G°_{H^-}$ for $HCo(dppe)_2$. The scheme makes use of the reduction potentials for the HCo(III/II) and HCo(II/I) couples (reactions 8 and 9), the pK_a (11.3) of $[HCo(dppe)_2(CH_3CN)]^{2+}$ in acetonitrile (reaction 10), and the $\Delta G°$ for the reduction of a proton to the hydride ion (reaction 11).[9] The sum of these steps, reaction 12, is hydride donation by $HCo(dppe)_2$, and the numerical value of $\Delta G°_{H^-}$ for this reaction can be determined by adding the $\Delta G°$ values for steps 8 through 11, as shown in eq 13. The value of $\Delta G°_{H^-}$ for $HCo(dppe)_2$ determined by this method is 49.1 kcal/mol.

$$HCo(dppe)_2 \leftrightarrows [HCo(dppe)_2]^+ + e^- \quad (8)$$

$$[HCo(dppe)_2]^+ + CH_3CN \leftrightarrows [HCo(dppe)_2(CH_3CN)]^{2+} + e^- \quad (9)$$

$$[HCo(dppe)_2(CH_3CN)]^{2+} \leftrightarrows [Co(dppe)_2]^+ + CH_3CN + H^+ \quad (10)$$

$$H^+ + 2e^- \rightarrow H^- \quad (11)$$

$$HCo(dppe)_2 \rightarrow [Co(dppe)_2]^+ + H^- \quad (12)$$

$$\Delta G°_{H^-(12)} = 23.06E°_{HCo(I/II)} + 23.06E°_{HCo(II/III)} + 1.37pK_{a(10)} + 79.6 \quad (13)$$

This result can be checked by comparison to the value determined by an alternate thermodynamic cycle. A $\Delta G°_{H^-}$ of 49.3 kcal/mol is calculated for $HCo(dppe)_2$ from the sequential protonation of $HCo(dppe)_2$ to form $[H_2Co(dppe)_2]^+$ (−31.3 kcal/mol), removal of H^- from $[H_2Co(dppe)_2]^+$ to form $[HCo(dppe)_2(CH_3CN)]^{2+}$ (65.1 kcal/mol), and deprotonation of $[HCo(dppe)_2(CH_3CN)]^{2+}$ to form $[Co(dppe)_2]^+$ (15.5 kcal/mol). All of these values were determined independently as discussed above, and this approach uses no electrochemical measurements. The two calculated $\Delta G°_{H^-}$ values for $HCo(dppe)_2$ (49.1 and 49.3 kcal/mol) are identical within our total estimated uncertainties for these measurements of ±2.5 kcal/mol.

By using thermodynamic cycles similar to those described above, it is possible to calculate all of the thermodynamic parameters shown in Table 3 (see Supporting Information for details). These values are ultimately determined by the open circuit potential of −0.83 V for the HCo(III/II) couple and the free energies associated with the deprotonation of $[HCo(dppe)_2(CH_3CN)]^{2+}$ and the hydride donor ability of $[H_2Co(dppe)_2]^+$ which were determined from equilibria 2 and 3, respectively. These equilibria were chosen because they are uncomplicated by the insolubility of $HCo(dppe)_2$ in acetonitrile, and both Co(III) species are relatively stable and easily purified. The reaction of $[H_2Co(dppe)_2]^+$ with tetramethylguanidine in benzonitrile provides a cross check on the free energy values for the hydride, hydrogen atom, and proton-transfer reactions of Table 3.

Discussion

Factors Influencing the pK_a Values of the Co−H Complexes. The free energy values for the successive deprotonation of $[H_2Co(dppe)_2]^+$ to $HCo(dppe)_2$ and $[Co(dppe)_2]^-$ are 31.3 kcal/mol (pK_a = 22.8) and 52.3 kcal/mol (pK_a = 38.1), respectively. This corresponds to a change of 15.3 pK_a units for these two sequential deprotonation reactions. This ΔpK_a is much larger than the value of 8.7 for the sequential deprotonation of the isoelectronic compound $H_2Fe(CO)_4$ in water.[22] Similarly, $H_3Re_3(CO)_{12}$ has been deprotonated sequentially to $[Re_3(CO)_{12}]^{3-}$ with $\Delta pK_{a1} = 7$ and $\Delta pK_{a2} = 15$.[23] The carbonyl ligands of $H_2Fe(CO)_4$ are good pi-acceptors, and as a consequence sequential deprotonation for this complex does not produce a large negative charge localized on the Fe atom. The diphosphine ligand, dppe, is not able to delocalize the negative charge as well as carbonyl ligands, and a larger negative charge is produced on the cobalt atom. As a result, the pK_a values as well as the ΔpK_a for $[H_2Co(dppe)_2]^+$ are significantly larger than that for $H_2Fe(CO)_4$.

From the data shown in Table 3, the effect of sequential oxidation on the Co−H cleavage reactions of $HCo(dppe)_2$ can also be assessed. The pK_a value of $HCo(dppe)_2$ decreases from 38.1 to 23.6 for the monocation and to 11.3 for the dication. The ΔpK_a values of ∼15 and 12 units, respectively, are somewhat smaller than those reported for $CpM(CO)_2(L)H$ hydrides (where M = Cr, Mo, and W, and L = CO or PR_3) and their oxidized partners, which are in the range of 20−25 pK_a units.[24,25] The pK_a values are useful in assessing the potential stability of an oxidized hydride to deprotonation. The fact that $[HCo(dppe)_2]^+$ is relatively stable to deprotonation probably contributes to the reversibility of the $HCo(dppe)_2/[HCo(dppe)_2]^+$ couple.

Factors Influencing the $\Delta G°_{H\cdot}$ Values of the Co−H Complexes. The successive homolytic bond cleavage reactions of $[H_2Co(dppe)_2]^+$ require 58.0 and 49.9 kcal/mol, respectively. These values indicate that the observed disproportionation of $[HCo(dppe)_2]^+$, reaction 1, is favored by approximately 8 kcal/mol. In addition, the sum of $\Delta G°_{H\cdot}$ for the two homolytic cleavage reactions is 107.9 kcal/mol as compared to a free energy of 103.6 kcal/mol for the homolytic cleavage of H_2 in acetonitrile.[9] This is consistent with the observed addition of H_2 to $[Co(dppe)_2]^+$ to form $[H_2Co(dppe)_2]^+$. This reaction can be reversed by purging solutions of $[H_2Co(dppe)_2]^+$ with nitrogen.

(22) Gamembeck, F.; Krumholz, P. *J. Am. Chem. Soc.* **1971**, *93*, 1909.
(23) Kaez, H. D. *Chem. Br.* **1973**, *9*, 344.
(24) Tilset, M. *J. Am. Chem. Soc.* **1992**, *114*, 2740−2741.
(25) (a) Ryan, O. B.; Tilset, M.; Parker, V. D. *J. Am. Chem. Soc.* **1990**, *112*, 2618−2626. (b) Skagestad, V.; Tilset, M. *J. Am. Chem. Soc.* **1993**, *115*, 5077−5083.

Values for the homolytic H−Co bond cleavage reactions have also been determined for each of the three oxidation states of $[HCo(dppe)_2]^{n+}$. Unlike the pK_a trends, the $\Delta G°_{H•}$ values do not show a regular correlation with oxidation state, and the decrease in $\Delta G°_{H•}$ with increasing charge actually appears to be relatively minor. For example, oxidation of $HCo(dppe)_2$ to $[HCo(dppe)_2]^+$ results in a 9−10 kcal decrease in the free energy, but further oxidation to form $[HCo(dppe)_2(CH_3CN)]^{2+}$ results in an increase in $\Delta G°_{H•}$ of approximately 3 kcal/mol. Three of the four homolytic bond cleavage reactions in Table 3 result in the formation of a metal centered radical as well as a hydrogen atom. The free energies associated with all of these reactions are larger than that observed for the homolytic cleavage of the bond for $[HCo(dppe)_2]^+$ which results in the formation of the low spin 16-electron complex, $[Co(dppe)_2]^+$. The formation of a metal-based radical appears to influence the free energy associated with the homolytic cleavage of the Co−H bond more than the oxidation state of the metal or the charge on the metal-hydride complex.

The data in Table 3 indicate that the homolytic cleavage of molecular hydrogen is thermodynamically favored by all three odd electron cobalt species, and the driving force increases in the order $[Co(dppe)_2(CH_3CN)]^{2+} < [HCo(dppe)_2]^+ < Co(dppe)_2$ with the latter two being nearly equal. The free energy values shown in Table 3 can be converted to enthalpies by correcting for the entropy contribution for the hydrogen atom in acetonitrile (approximately 4.6−4.8 kcal/mol).[7d,9] This correction is based on the assumptions that $S°$ for the hydride and that for its conjugate radical are equal and that the entropy of solvation for the hydrogen atom and that for the hydrogen molecule are also equal. The enthalpy values of 64 kcal/mol for $HCo(dppe)_2$ and 63 kcal/mol for $[H_2Co(dppe)_2]^+$ can be compared to the values of 65 and 67 kcal/mol reported previously for $HCo(CO)_3PPh_3$ and $HCo(CO)_4$, respectively.[7d,e]

Factors Influencing the $\Delta G°_{H^-}$ Values of the Co−H Complexes. The hydride donor ability of the two cationic species, $[H_2Co(dppe)_2]^+$ and $[HCo(dppe)_2]^+$, are 65.1 and 59.7 kcal/mol, respectively. These values lie within the range (67−51 kcal/mol) previously observed for $[HNi(diphosphine)_2]^+$ complexes.[3,4,10] The neutral hydride, $HCo(dppe)_2$, is a much more powerful hydride donor than either of these by 10−15 kcal/mol, and its hydride donor value of 49.1 kcal/mol is comparable to the value observed for $[HPt(dppe)_2]^+$ (52.5 kcal/mol).[3] It appears that changing from Ni to Co has approximately the same effect on hydride donor potentials as changing from Ni to Pt for isoelectronic and isostructural species. In previous work on $[HNi(diphosphine)_2]^+$ complexes, we have shown that a linear free energy relationship exists between the hydride donor ability of a complex ($\Delta G°_{H^-}$) and the potential of the (d^8/d^9) couple of the conjugate hydride acceptor, $[Ni(diphosphine)_2]^{2+}$.[10] The calculated $\Delta G°_{H^-}$ value of 49.1 kcal/mol for $HCo(dppe)_2$ agrees well with the value of 47.7 kcal/mol calculated using the equation for the best-fit line for the Ni complexes. This result suggests that it may be possible to extend the relationship developed previously for $[HNi(diphosphine)_2]^+$ complexes to provide a useful estimate of the hydricity of other five-coordinate first row metal-hydride complexes.

Summary and Conclusions

The major objective of this research was to demonstrate that comprehensive thermodynamic schemes can be developed for transition metal-dihydride systems in a manner similar to those developed previously for monohydride systems. Our results for the $[H_2Co(dppe)_2]^+$ system selected for this study are summarized in Figure 3. The figure illustrates the relationships between the various thermodynamic properties of the hydrides (and non-hydrides) and helps shift the perspective from a single pK_a, $\Delta G°_{H•}$, or $\Delta G°_{H^-}$ measurement for a single compound to one of an integrated system of compounds that are interrelated by the various simple reactions shown. The relationships of Figure 3 are very useful in developing a quantitative understanding of how the cobalt complexes will respond to changes in the acidity or basicity of the environment, the introduction of a hydrogen atom or hydride acceptor, or a change in the electrochemical potential of the solution. We believe these responses are best understood when viewing the complexes as part of a total thermodynamic system. The approach developed here suggests that it should be possible to obtain detailed thermodynamic descriptions of the metal−hydrogen bond in a variety of metal-hydride complexes with nonlabile ligands, including polyhydride and polynuclear systems.

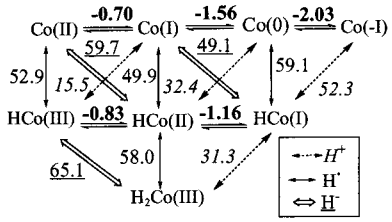

Figure 3. Thermodynamic relationships between $[Co(dppe)_2]^{n+}$ and $[H_x-Co(dppe)_2]^{m+}$ where $n = -1, 0, 1, 2$, $x = 1, 2$, and $m = 0, 1, 2$. Numbers in bold are reduction potentials in volts vs Fc. Numbers near arrows are $\Delta G°$ values for the indicated proton, hydrogen atom, or hydride-transfer reaction in kcal/mol.

Experimental Section

Materials and Instrumentation. ^1H NMR and ^{31}P NMR spectra were recorded on a Varian Unity 500 MHz spectrometer. ^1H chemical shifts are reported relative to tetramethylsilane using residual solvent protons as a secondary reference. A capillary filled with phosphoric acid was used as an external reference for ^{31}P NMR spectra. All ^{31}P NMR spectra were proton decoupled. Solvent suppression studies were recorded on a Bruker AM-400 MHz spectrometer using a presaturation technique. In experiments where accurate integration of the hydride was necessary, spectra were collected using a repetition rate of 0.100 s with a tip angle of 43° to allow for the relaxation of the hydride which has a $T_1 = 0.135$ s. Infrared spectra of Nujol mulls were recorded on a Nicolet 510P spectrometer. Electron spin resonance spectra were recorded on a Varian E109 X-band spectrometer. Air-sensitive solutions of 2 mM concentration in acetonitrile were transferred to an EPR tube under a N_2 atmosphere in a glovebox.

All electrochemical experiments were carried out under an atmosphere of N_2 in 0.3 M Bu_4NBF_4 solutions of benzonitrile or acetonitrile. Cyclic voltammetry studies were carried out on a Cypress Systems computer aided electrolysis system. The working electrode was a glassy carbon disk (2 mm diameter). The counter electrode was a glassy carbon rod. An Ag/AgCl reference electrode was used to fix the potential. Ferrocene was used as an internal standard, and all potentials are referenced to the ferrocene/ferrocenium couple. Chronopotentiometric studies were carried out using the same electrodes and instrumentation.

1,2-Bis(diphenylphosphinoethane) (dppe), cobalt powder, ferrocenium hexafluorophosphate, ferrocenium tetrafluoroborate, sodium borohydride, tetrafluoroboric acid, and tetrabutylammonium tetrafluoroborate were purchased from Aldrich Chemical Co. Acetonitrile and methylene chloride were dried by distillation from calcium hydride under nitrogen.

Tetrahydrofuran, toluene, and diethyl ether were dried by distillation from sodium benzophenone ketyl under nitrogen. Absolute ethanol and reagent grade benzonitrile were used as received. All solvents were purged with nitrogen for 15 min before use. Acetonitrile-d_3, benzene-d_6, and acetone-d_6 were freeze−pump−thawed, dried over molecular sieves, and stored under inert atmosphere in a glovebox. All reactions were performed using standard Schlenk techniques under nitrogen. $[Co(CH_3CN)_6][BF_4]_2$[26] and $[Co(dppe)_2(CH_3CN)][BF_4]_2$[13] were prepared according to literature methods. Synthetic methods and elemental analyses have been reported for the synthesis of $HCo(dppe)_2$,[11a] $[HCo(dppe)_2][BPh_4]$,[12] $[HCo(dppe)_2(CH_3CN)][BPh_4]_2$,[12] $[Co(dppe)_2][BPh_4]$,[27] and $[H_2Co(dppe)_2][ClO_4]$.[11a] The following synthetic methods have been slightly modified from the reported procedures. The spectroscopic, electrochemical, and structural studies indicate that they are the same complexes as those identified earlier.

$HCo(dppe)_2$. A slurry of $[Co(dppe)_2(CH_3CN)](BF_4)_2$ (4.92 g, 4.6 mmol) in ethanol (200 mL) was heated to 65 °C. A solution of sodium borohydride (0.522 g, 13.8 mmol) in 95% aqueous ethanol was added slowly over an hour, which resulted in the formation of a red precipitate. The slurry was stirred overnight. The precipitate was collected by filtration and washed with ethanol (2 × 30 mL) to remove excess sodium borohydride. The crude product was recrystallized from a mixture of tetrahydrofuran and ethanol. Yield: 58% (2.29 g). ^{1}H NMR (benzene-d_6): δ 6.90−7.40 (m, 40H, P*Ph*$_2$), 2.15 (s, 8H, P*CH*$_2$*CH*$_2$), −14.9 (quintet, 1H, Co−*H*). ^{31}P NMR (benzene-d_6): δ 72.9 (s). IR (Nujol mull): $\nu_{Co-H} = 1882$ cm^{-1}. $E°$ (II/I) = −1.16 V.

$[HCo(dppe)_2(CH_3CN)](PF_6)_2$. A solution of ferrocenium hexafluorophosphate (0.537 g, 1.64 mmol) in acetonitrile (100 mL) was added to a slurry of $HCo(dppe)_2$ (0.700 g, 0.82 mmol) in acetonitrile (150 mL). The resulting light brown solution was stirred for 3 days. The solvent was removed in vacuo to give an orange-brown solid. The solid was washed with toluene (4 × 25 mL) to remove ferrocene. The crude product was recrystallized from a mixture of methylene chloride and ethanol to give a yellow solid. Yield: 74% (0.72 g). This procedure was repeated with ferrocenium tetrafluoroborate to produce the tetrafluoroborate derivative. ^{1}H NMR (acetonitrile-d_3): δ 6.67−7.59 (m, 5H, P*Ph*$_2$), 2.39 (s, 4H, P*CH*$_2$*CH*$_2$), 3.00 (s, 4H, P*CH*$_2$*CH*$_2$), −21.1 (quintet, 1H, Co−*H*). ^{31}P NMR (acetonitrile-d_3): δ 66.6 (s). IR (Nujol mull): $\nu_{Co-H} = 1977$ cm^{-1}, $\nu_{C-N} = 2282$ cm^{-1}. $E°$ (II/I) = −1.16 V.

$[H_2Co(dppe)_2](BF_4)$. Zinc powder (0.580 g, 8.87 mmol) was added to a solution of $[Co(dppe)_2(CH_3CN)](BF_4)_2$ (0.950 g, 0.880 mmol) in acetonitrile (100 mL). The solution was stirred for 36 h. Hydrogen gas was bubbled through the solution for 15 min. The resulting orange solution was filtered to remove the excess zinc. Diethyl ether which had been purged with hydrogen was added to the solution to precipitate a yellow solid that was collected by filtration and was washed with water (2 × 20 mL) followed by H_2 saturated diethyl ether (2 × 30 mL). Yield: 34% (0.260 g). ^{1}H NMR (acetonitrile-d_3): δ 6.17−7.93 (m, 40H, C_6H_5), 3.29−3.36 (d, br, 4H, PC*H*$_2$C*H*$_2$), 2.26 (s, br, 4H, PC*H*$_2$C*H*$_2$), δ −13.2 (m, 2H, Co*H*). ^{31}P NMR (acetonitrile-d_3): 69.7 (s, br), 80.5 (s, br).

$[HCo(dppe)_2](BF_4)$. A solution of $HCo(dppe)_2$ (0.290 g, 0.339 mmol) in tetrahydrofuran (80 mL) was added to a solution of $[HCo(dppe)_2CH_3CN](PF_6)_2$ (0.395 g, 0.333 mmol) in acetonitrile (30 mL). The resulting brown solution was stirred for 18 h and then filtered. The solvent was removed in vacuo. The golden brown solid was recrystallized from a mixture of methylene choride and ethanol. Yield: 34%. IR (Nujol mull): $\nu_{Co-H} = 1874$ cm^{-1}. $E°$ (II/I) = −1.16 V. EPR (CH_3CN, 25 °C): $g = 2.1$, d, $A = 80$ G. (It has not been established whether the observed doublet results from coupling to the hydride or to a phosphorus atom.)

$[Co(dppe)_2](BF_4)$. Zinc powder (0.287 g, 4.40 mmol) was added to a solution of $[Co(dppe)_2(CH_3CN)](BF_4)_2$ (0.470 g, 0.440 mmol) in acetonitrile (100 mL). The solution was stirred for 36 h. The resulting dark brown solution was filtered to remove the excess zinc. The solvent was removed in vacuo. The solid was washed with water (2 × 20 mL) followed by a diethyl ether wash (2 × 30 mL). The resulting brown solid is unstable; attempts at recrystallization were unsuccessful. The yield of the crude product was 71.3% (0.308 g). ^{1}H NMR (acetonitrile-d_3): δ 7.08−7.30 (m, P*Ph*$_2$), 2.32 (s, 8H, P*CH*$_2$*CH*$_2$). No ^{31}P NMR signal was detected. $E°$ (II/I) = −0.607 V, $E°$ (I/0) = −1.62 V, $E°$ (0/−I) = −2.07 V.

pK_a Measurement for $[HCo(dppe)_2(CH_3CN)](BF_4)_2$. Aliquots (0.5 mL each) of a 1.28×10^{-2} M solution of $[HCo(dppe)_2(CH_3CN)](BF_4)_2$ (0.051 g) in acetonitrile-d_3 were syringed into each of five NMR tubes. This was followed by aliquots of different volumes of a 0.286 M solution of anisidine in acetonitrile-d_3 and a 0.286 M solution of anisidinium tetrafluoroborate in acetonitrile-d_3 to produce a constant volume of 1.0 mL. The solutions were monitored by ^{1}H NMR for 6 days until the ratio of $[HCo(dppe)_2(CH_3CN)](BF_4)_2$ to $[Co(dppe)_2](BF_4)$ remained constant. The ratio of the concentrations of the two metal complexes was calculated by integration of the ^{1}H NMR signals of the methylene groups of the dppe ligands. The reverse reaction was studied by mixing a 2.5×10^{-2} M solution of $[Co(dppe)_2](BF_4)$ in acetonitrile-d_3 (0.5 mL) and 0.250 M solutions of anisidine (0.25 mL) and anisidinium tetrafluoroborate (0.25 mL) in acetonitrile-d_3. The solution was monitored by ^{1}H NMR for 6 days, until the ratio of products remained constant.

pK_a Measurement for $[H_2Co(dppe)_2](BF_4)$. Aliquots (0.5 mL each) of a 1.48×10^{-2} M solution of $[H_2Co(dppe)_2](BF_4)$ in benzonitrile were syringed into each of four NMR tubes followed by known amounts of tetramethylguanidine (TMG) in benzonitrile to produce a total volume of 0.65 mL. CD_3CN (0.07 mL) was added to each NMR tube to provide a lock signal. The solutions were monitored by solvent suppression ^{1}H NMR for 4 days until the ratio of products remained constant as determined by integration of the hydride ^{1}H NMR resonances. To study this reaction in the reverse direction, aliquots (0.4 mL) of a 2.2×10^{-3} M solution of $HCo(dppe)_2$ in benzonitrile were syringed into three NMR tubes, and aliquots of different known volumes of 0.252 M TMG and 0.252 M $[TMGH](BF_4)$ solutions in benzonitrile were added to give a constant volume of 0.65 mL. The solutions were monitored by ^{1}H NMR for 4 days until the ratio of the products remained constant.

Equilibrium Studies of the $[H_2Co(dppe)_2](BF_4)$/$[HCo(dppe)_2(CH_3CN)](BF_4)_2$ System with Hydrogen and Base. Aliquots (0.4 mL) of a 6.4×10^{-2} M solution of $[H_2Co(dppe)_2](BF_4)$ in acetonitrile-d_3 were syringed into each of four NMR tubes, and various aliquots of 1.27 M solutions of 2,4-dichloroaniline and 2,4-dichloroanilinium tetrafluoroborate in acetonitrile-d_3 were added to produce a constant volume of 0.8 mL. The solutions were purged with hydrogen (and each day afterward) and monitored by ^{1}H NMR for 8 days until the ratio of $[H_2Co(dppe)_2](BF_4)$ to $[HCo(dppe)_2CD_3CN][BF_4]_2$ remained constant as determined by integration of the hydride ^{1}H NMR signals. The reverse reaction was studied by adding aliquots (0.4 mL) of a 1.28×10^{-2} M solution of $[HCo(dppe)_2CD_3CN][BF_4]_2$ in acetonitrile-d_3 to five NMR tubes. Various aliquots of 0.256 M solutions of 2,4-dichloroaniline and 2,4-dichloroanilinium tetrafluoroborate (0.0830 g) in acetonitrile-d_3 were then added to give a constant volume of 0.8 mL. All of the NMR tubes were purged with hydrogen, and the solutions were monitored by ^{1}H NMR for 8 days, until the ratio of the products remained constant.

X-ray Diffraction Studies. Single-crystal X-ray data for three complexes were collected at low temperature, ca. 150 K, on a Siemens SMART CCD diffractometer using Mo Kα radiation ($l = 0.71073$ Å). An arbitrary hemisphere of data to 0.68 Å resolution was collected for each sample. Each data frame was 0.3° in ω; frames were a correlated scan comprised of two exposures at half the total scan time. All data were corrected for Lorentz and polarization effects, as well as for absorption. Structure solution was by direct methods. Anisotropic thermal parameters were refined for all non-hydrogen atoms. All

(26) Hathaway et al. *J. Chem. Soc*. **1962**, 2444−2448.
(27) Nobile, C.; Rossi, M.; Sacco, A. *Inorg. Chim. Acta* **1971**, 698−700.

Table 4. Crystallographic Data for $HCo(dppe)_2$, $[HCo(dppe)_2CH_3CN](PF_6)_2$, $[H_2Co(dppe)_2](BF_4)$, and $[Co(dppe)_2CH_3CN](BF_4)_2$

	$HCo(dppe)_2$	$[HCo(dppe)_2CH_3CN](PF_6)_2 \cdot (CH_2Cl_2)$	$[H_2Co(dppe)_2](BF_4) \cdot (CH_3)_2CO$	$[Co(dppe)_2CH_3CN](BF_4)_2 \cdot (CH_3)_2CO$
empirical formula	$C_{52}H_{49}CoP_4$	$C_{55}H_{54}Cl_2CoF_{12}NP_6$	$C_{55}H_{56}BCoF_4OP_4$	$C_{57}H_{57}B_2CoF_8NOP_4$
formula mass, amu	856.72	1272.64	1002.62	1128.47
cryst syst	monoclinic	monoclinic	monoclinic	orthorhombic
space group	$P2_1/n$	$P2_1/n$	$P2_1/n$	$P2_12_12_1$
a (Å)	9.8888(4)	19.4102(15)	13.779(2)	11.7261(5)
b (Å)	20.7973(10)	16.9353(13)	19.320(2)	20.6176(9)
c (Å)	20.9906(10)	20.121(2)	18.595(2)	22.2925(10)
α (deg)	90	90	90	90
β (deg)	92.2570(10)	115.407(2)	102.225(15)	90
γ (deg)	90	90	90	90
V (Å^3)	4313.6(3)	5974.3(8)	4837.9(11)	5389.5(4)
Z	4	4	4	4
T (K)	143(2)	141(2)	143(2)	293(2)
R index[a] ($I > 2\sigma(I)$)	R1 = 0.0463, wR2 = 0.1144	R1 = 0.0947, wR2 = 0.2447	R1 = 0.0618, wR2 = 0.1321	R1 = 0.0759, wR2 = 0.1099
R index[a] (all data)	R1 = 0.0715 wR2 = 0.1248	R1 = 0.1486 wR2 = 0.2728	R1 = 0.1305 wR2 = 0.1591	R1 = 0.2299 wR2 = 0.1497
weighting coeff[b]	$a = 0.0670$, $b = 1.1366$	$a = 0.1597$, $b = 0$	$a = 0.0709$, $b = 0$	$a = 0.0418$, $b = 0$
GOF[c] on F^2	1.068	1.044	0.938	0.927

[a] $R1 = \sum||F_o| - |F_c||/\sum|F_o|$; $wR2 = [\sum w(F_o^2 - F_c^2)/\sum w(F_o^2)^2]^{1/2}$. [b] $W^{-1} = [\sigma^2(F_o^2) + (ap)^2 + bp]$, where $P = (F_o^2 + 2F_c^2)/3$. [c] $GOF = S = [\sum w(F_o^2 - F_c^2)/(M - N)]^{1/2}$, where M is the number of reflections, and N is the number of parameters refined.

hydrides were located by a difference Fourier map but were freely refined in subsequent cycles of least-squares refinement. Selected details of the structure solutions and refinements are given in Table 4 , and comments for specific compounds are given in the following paragraphs.

$HCo(dppe)_2$. Crystals were grown from a saturated solution of benzene-d_6. This complex crystallized in the centrosymmetric space group $P2_1/n$. Data were collected at 145 K using 30 s scans. There was no disorder.

$[HCo(dppe)_2(CH_3CN)](PF_6)_2$. Crystals were grown from methlyene chloride and ethanol. The complex crystallized in the centrosymmetric space group $P2_1/n$. Data were collected at 145 K using 30 s scans. Two molecules of solvent are present in the crystal lattice. One molecule of methylene chloride was disordered over two sites. The volume occupied by a second highly disordered methylene chloride molecule was analyzed using SQUEEZE.[28] This program found electron density equivalent to 244 electrons which is close to six molecules of methylene chloride. This electron density was removed from the file of observed f's prior to subsequent cycles of least squares refinement.

$[H_2Co(dppe)_2](BF_4)$. Crystals were grown from a saturated solution of acetone-d_6. Data were collected at 145 K using 30 s scans. This complex crystallized in the centrosymmetric space group $P2_1/n$. A molecule of acetone was present in the crystal lattice. There was no disorder.

$[Co(dppe)_2CH_3CN][BF_4]_2$ (4). Crystals were grown from acetone-d_6. Data were collected at 145 K using 30 s scans. A molecule of acetone was present in the crystal lattice. There was a small amount of disorder in the BF_4 molecule.

Acknowledgment. This research was supported by the National Science Foundation. D. L. DuBois would also like to acknowledge the support of the United States Department of Energy, Office of Basic Energy Sciences, Division of Chemical Sciences.

Supporting Information Available: Complete details of the X-ray diffraction studies on $HCo(dppe)_2$, $[HCo(dppe)_2(CH_3CN)](PF_6)_2$, $[H_2Co(dppe)_2](BF_4)$, and $[Co(dppe)_2(CH_3CN)](BF_4)_2$, and details of the calculations of $\Delta G°$ values (PDF). This material is available free of charge via the Internet at http://pubs.acs.org.

JA0122804

(28) Spek, A. L. SQUEEZE is a routine included in *PLATON, A Multipurpose Crystallographic Tool*; Utrecht University: Utrecht, The Netherlands, 2001.